Diffusion-weighted imaging in musculoskeletal radiology—clinical applications and future directions

Nicholas Bhojwani[1]*, Peter Szpakowski[2]*, Sasan Partovi[2], Martin H. Maurer[3], Ulrich Grosse[2,4], Hendrik von Tengg-Kobligk[3], Lisa Zipp-Partovi[5], Nathan Fergus[2], Christos Kosmas[2], Konstantin Nikolaou[4], Mark R. Robbin[2]

[1]Department of Radiology, Vanderbilt University Medical Center, Nashville, Tennessee; [2]Department of Radiology, University Hospitals Case Medical Center, Case Western Reserve University, Cleveland, Ohio, USA; [3]Institute of Diagnostic, Interventional and Pediatric Radiology, Inselspital University Hospital Bern, Freiburgstrasse, Bern 3010, Switzerland; [4]Department of Diagnostic and Interventional Radiology, University Hospital Tübingen, Tübingen, Germany; [5]Department of Pediatrics, Rainbow Babies and Children's Hospital, University Hospitals Case Medical Center, Cleveland, Ohio, USA

*These authors contributed equally to this work.

Correspondence to: Mark R. Robbin, MD. Department of Radiology, University Hospitals Case Medical Center, Case Western Reserve University, Cleveland, Ohio, USA. Email: mark.robbin@uhhospitals.org.

Abstract: Diffusion-weighted imaging (DWI) is an established diagnostic tool with regards to the central nervous system (CNS) and research into its application in the musculoskeletal system has been growing. It has been shown that DWI has utility in differentiating vertebral compression fractures from malignant ones, assessing partial and complete tears of the anterior cruciate ligament (ACL), monitoring tumor response to therapy, and characterization of soft-tissue and bone tumors. DWI is however less useful in differentiating malignant *vs.* infectious processes. As of yet, no definitive qualitative or quantitative properties have been established due to reasons ranging from variability in acquisition protocols to overlapping imaging characteristics. Even with these limitations, DWI can still provide clinically useful information, increasing diagnostic accuracy and improving patient management when magnetic resonance imaging (MRI) findings are inconclusive. The purpose of this article is to summarize recent research into DWI applications in the musculoskeletal system.

Keywords: Diffusion-weighted imaging (DWI); magnetic resonance imaging (MRI); PET/MRI; musculoskeletal neoplasms; inflammatory conditions; therapy assessment

Introduction

Even though initial research into diffusion-weighted imaging (DWI) applications focused on the central nervous system (CNS) (1-4), there now is a growing amount of research extending to other systems. Applications of DWI in the musculoskeletal system have come to include assisting in differentiating vertebral compression fractures *vs.* malignant fractures (5), degenerative changes (6,7), monitoring tumor response to therapy (8), differentiating degenerative *vs.* infectious processes (9), malignant *vs.* infectious processes (10), and characterization of soft-tissue and bone tumors (11). The goal of this article is to provide a brief overview of the recent advancements and studies in the applications of DWI to the musculoskeletal system in the context of the authors' institutional experiences.

Image acquisition and interpretation

The single shot echo planar imaging (SS-EPI) technique is the most commonly used sequence in DWI, providing

not only rapid image acquisition but reduced motion artifacts (12). Although the mechanics behind DWI have not been elucidated entirely (13), it is a non-invasive method which measures the Brownian motion of water in its microscopic environment. This principle is exploited to detect and monitor the cellularity of a variety of pathologies. The signal obtained reflects the water content of the tissue, which is influenced by both perfusion and diffusion making image interpretation difficult. A diffusion weighted image is created by applying diffusion sensitizing gradients to a T2-weighted image, where the parameters of the sensitizing gradient are determined by the b value. With a b value of 0, the image appears as a T2-weighted image and a progressive increase in the b value begins to suppress the perfusion effect, with only highly cellular tissues remaining bright at high b values (13). A hyperintense signal on DWI corresponds to an area where water motion is restricted and is not able to move out of the image plane. Because extracellular fluid motion is less restricted in comparison to intracellular fluid motion, more extracellular fluid will result in decreased signal. In contrast, an increased signal correlates to increased cellularity of the tissue because intracellular fluid motion is impeded by organelles (11,14).

In conjunction with DWIs, apparent diffusion coefficient maps (ADC) are sometimes given, quantify the effect of diffusion restriction. ADC calculation requires at least two DWIs at different b values and in contrast to DWI, stationary water appears hypointense on ADC maps (i.e., reduced diffusion) and hyperintense where there is increased water diffusion. ADC values in cells are much lower than in free standing water because cellular structures impede the diffusion of water. With low b values, the perfusion component accounts for a larger proportion of the signal intensity on ADC maps whereas diffusion dominates at higher b values. These can be reported as ADC_{slow} and ADC_{fast} components but generally, only a total ADC value is given (13).

For proper interpretation of DWIs and ADC maps, clinical correlation is essential. Tumors generally have restricted diffusion compared to healthy tissues due to enlarged nuclei and increased cellularity resulting in decreased extracellular volumes. The restricted diffusion leads to increased signal on DWI and decreased signal on ADC map. Depending on the features of the malignancy and the treatment response, this pattern may change in the course of the pathology. Rapidly growing tumors can outgrow their vascular supply or treatment of tumors can lead to necrosis, causing decreased signal intensity on high b value images and increased ADC values. Certain tissues with long T2 relaxation times can cause increased signal on DWI images even though they are not due to decreased diffusion. This process is termed the "T2-shine through effect" and leads to an increased signal on both, DWI and ADC maps (13), therefore comparison of the two is essential.

Malignancies of soft-tissue and bone

Morphological magnetic resonance imaging (MRI) techniques are applied in the workup of certain soft-tissue tumors and characteristic imaging findings are helpful to narrow down the differential diagnosis. Investigations using DWI as a functional MR sequence have been focusing on developing qualitative and quantitative criteria for musculoskeletal tumors. One study found that defining imaging characteristics on MRI that may differentiate chondrosarcomas from chondroblastic osteosarcomas and other osteosarcomas is difficult due to overlapping imaging features (11). Tumor heterogeneity causes ADC values to be variable depending on the region of interest selected, with areas of higher cellularity and stroma demonstrating low ADC values (14). Although tumor heterogeneity on imaging suggests malignancy, it should not be considered a prerequisite (14). In the majority of cases histopathological confirmation is required. However, the tumor heterogeneity reflected by DWI and corresponding ADC maps may be helpful for planning of image guided biopsy (*Figure 1*).

Setting ADC cut-off values for benign and malignant tumors has also proven to be difficult which is in part due to variability in image acquisition protocols and technical specifications between vendors (15). A cut-off value of 1.34×10^{-3} mm^2/s proposed by one study (16) showed a sensitivity of 91% and specificity of 94% in differentiating between malignant and benign soft-tissue tumors. For cystic lesions, using a mean ADC value greater than 2.5×10^{-3} mm^2/s led to a sensitivity of 80% and specificity of 100% (17), although the use of different imaging protocols can achieve higher ADC values of soft-tissue tumors (15). ADC values are usually lower in malignant tumors compared to benign tumors, but the overlap in values has made it impossible at this point to define ADC cut-offs with high sensitivity or specificity thus limiting its diagnostic value (15,18,19). Nevertheless, the features suggesting malignancy on DWI are areas of hyperintensity seen at high b values and corresponding hypointensity on ADC map (20).
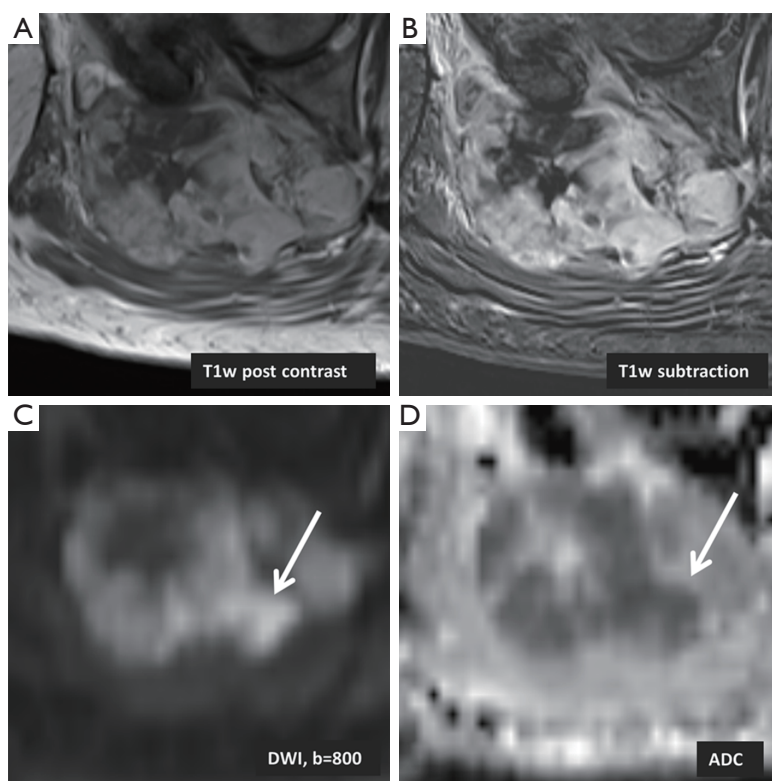
Figure 1 A 63-year-old female with a myxoid liposarcoma. Large parts of the tumor mass show strong contrast enhancement (A; B, with subtraction); the diffusion weighted imaging displays high signal especially in a nodular medial part of the tumor (C, white arrow) with corresponding low signal on the ADC map (D, white arrow). This part of the tumor contains the highest cellularity and should be chosen as a target for biopsy.

Research in the use of whole body DWI with background body signal suppression in localization of metastatic bone lesions and staging of tumors is showing good results and clinical applications are still being explored (21-23). DWI in comparison to positron emission tomography (PET) and scintigraphy has shown to be more effective in detecting metastatic bone tumors (24) while avoiding the need for isotopes which are in short supply (25). One study conducted a meta-analysis of 495 patients (26) and showed that whole-body DWI is sensitive but not specific in detecting bone lesions. Whole-body MRI eliminates exposure to high-doses of radiation, an important consideration especially if the patient is to undergo frequent imaging and is young (27). DWI has been shown to as effective or more effective in detecting metastatic prostate cancer, breast cancer and multiple myeloma in comparison to STIR-based protocols (28,29). Tumor localization when, conducting whole body diffusion, can be improved with overlay of anatomical imaging (*Figure 2*). Even though superimposing anatomical imaging on DWI images might be helpful for the clinician, it does not increase tumor detection rates (30).

The most common primary malignant tumor of the bone is intramedullary osteosarcoma (11). Yakushiji *et al*. (11) found that DWI may be more effective than gadolinium enhanced MRI in differentiating chondroblastic osteosarcomas and other osteosarcomas. Gadolinium enhanced MRI is important because the large chondroid component can make it difficult to biopsy appropriate regions containing malignant tumor cells (31,32). Missing chondroblastic osteosarcomas is not only impairing patient management but eventually clinical outcome. Patients with chondrosarcoma have a 5-year survival rate of 72.6% when they receive appropriate treatment (33) whereas the 5-year survival rate for chondroblastic osteosarcomas is around 60% (34). MRI can assist in diagnosis of chondroblastic osteosarcoma (35), however, the septonodular and peripheral rim enhancement pattern often found in chondroblastic osteosarcomas can also be found in other chondroid matrix-forming tumors (11,36). In the specimens studied by Yakushiji *et al*. (11), a heterogeneous pattern of MR enhancement was found in all chondroblastic osteosarcomas and other types of
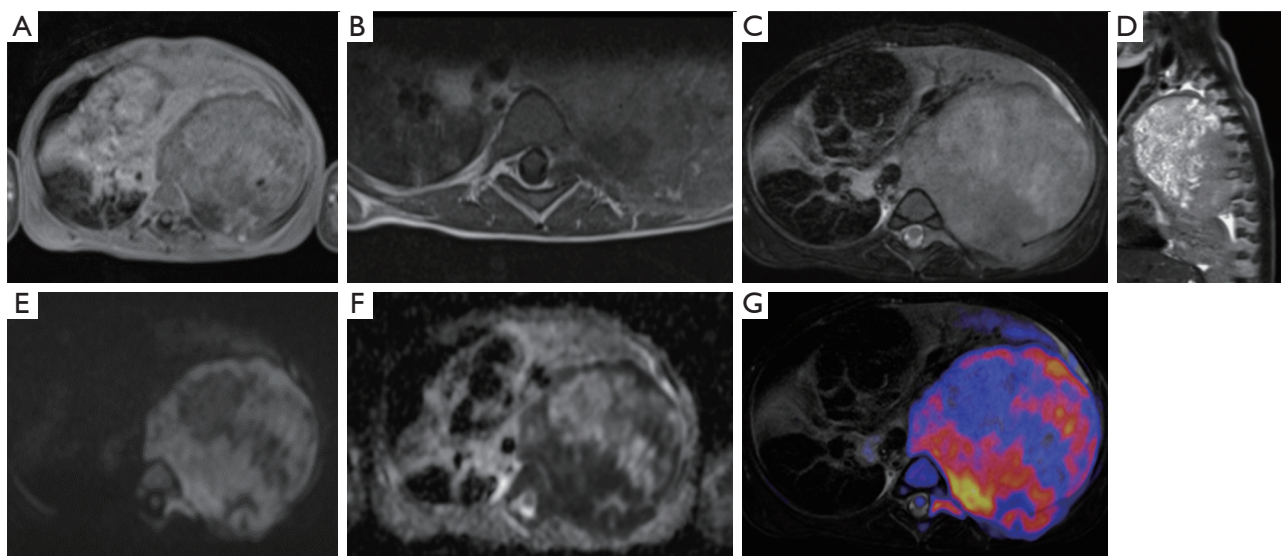
Figure 2 MR of a 4-year-old male patient with left thoracic Ewing sarcoma, originating from the 7th rib with the following images: (A) T1w VIBE post gadolinium axial; (B) T1w TSE fat-saturated axial; (C) T2w TSE fat-saturated axial; (D) T2w HASTE sagittal; (E) DWI with b=1,000 axial; (F) corresponding ADC map axial; (G) fusion of T2w TSE fat-saturated axial + color coded DWI with b=1,000 axial. Images demonstrate mediastinal shift to the right site with left lung atelectasis, invasion of the left main bronchus, left lung, and posterior thoracic wall. Furthermore, invasion of the neuroforamina at T5-6, T6-7 and T7-8 levels and the central canal without cord compression is well appreciated on the fused images. The remainder of unaffected left lung is collapsed. Please note the heterogeneity of the tumor with regard to cellularity DWI and ADC images. MR, magnetic resonance; DWI, diffusion-weighted imaging; ADC, apparent diffusion coefficients.

osteosarcoma, but was found in only 16.7% of chondrosarcoma cases. Minimum ADC values of osteosarcomas (n=17) was found to be $(0.84\pm0.15) \times 10^{-3}$ mm^2/s while chondroblastic osteosarcomas (n=5) and chondrosarcomas (n=18) had minimum ADC values of $(1.24\pm0.20) \times 10^{-3}$ and $(1.64\pm0.20) \times 10^{-3}$ mm^2/s respectively. Even though the population size was small, the use of DWI in differentiating osteosarcomas from chondroblastic osteosarcomas and chondrosarcomas provided useful information based on the results of this study. Increased diagnostic accuracy may be possible if DWI is used in conjunction with morphological gadolinium enhanced MRI (11).

Bone marrow infiltration can be difficult to interpret because of the composition changes that occur with normal bone marrow over time. Yellow marrow is composed largely of adipose cells and its extent increases as a person ages. This occurs in a peripheral to central manner (37). Red marrow has increased water content and cellularity due to hematopoiesis. The bone marrow may change from yellow to red or it can be infiltrated by malignant cells (38,39). In normal yellow marrow, characteristic DWI findings include low ADC values seen along with signal suppression at higher b values on DWI (13). Red and yellow marrow can be mixed

in the intramedullary space and when yellow is interspersed within red marrow, it is called islands of yellow marrow (37). This is an important consideration because medullary bone can appear to be heterogeneous on MRI and DWI. Replacement of bone marrow by malignant cells results in low ADC values (due to increased cellularity), however, increased signal can be seen at high b-value images (13). One study (40) investigated lymphomas infiltrating iliac bones and found that the use of DWI in conjunction with T1w spin echo results in a sensitivity of 77% and specificity of 92.5%. Although malignant tumors demonstrate high DWI signals and low ADC values, the study found red marrow can also demonstrate high signal intensity on DWI. It was also demonstrated in lymphomas infiltrating the iliac bone that T1-weighted images and STIR together provided a sensitivity and specificity of 85% and 97% respectively (40). Due to tendency of DWI to poor image quality and lower sensitivity and specificity, they suggested that bone lymphomas should be assessed using STIR and T1-weighted sequences. As in osteosarcomas, DWI can still play a role in whole-body imaging for localization of metastatic lesions and monitoring of tumor burden (21).

DWI may be helpful in differentiating between chronically expanding hematomas (CEH) and malignant soft tissue tumors (14). The term CEH was defined as a hematoma which ruptures and continues to grow for more than 1 month (41). On T1- and T2- weighted images, CEH can appear as a heterogeneous mass with a hypointense peripheral rim (42). Hemoglobin and red blood cell age found within the hematomas influence diffusion properties resulting in a heterogenous appearing mass on DWI (43), an important factor when considering intravascular blood and hemorrhagic components of the lesion (14). Calculating ADC maps, it was found that the mean ADC values of CEH [$(1.55\pm0.121) \times10^{-3}$ mm^2/s] compared to malignant soft-tissue masses [$(0.139\pm0.129) \times10^{-3}$ mm^2/s] was significantly higher. They concluded that ADC values can be helpful to differentiate CEH from malignant soft-tissue masses (14).

Benign fibrous and fibrohistiocytic tumors are soft-tissue tumors which are seen in different age groups (44). They can demonstrate characteristic features although it is possible for features of benign and malignant tumors to overlap resulting in misdiagnosis (45). Costa *et al.* (44) studied patients with histologically confirmed fibroblastic/myofibroblastic/fibrohistiocytic soft tissue tumors who were grouped according to the WHO classification scheme as benign, intermediate and malignant. Comparison of the perfusion-insensitive diffusion coefficient showed a statistically significant difference between benign/intermediate [$(1.56\pm0.25) \times10^{-3}$ mm^2/s] and malignant tumor groups [$(0.89\pm0.15) \times10^{-3}$ mm^2/s]. As previously discussed, overlap between ADC values is possible but the additional information from this sequence may allow a more comprehensive analysis of the lesion.

Knee injuries

MRI is frequently used to assess the soft-tissue components of the knee post injury. A recent study compared ADC mapping to MRI morphology imaging of the knee in partial and complete anterior cruciate ligament (ACL) tears (46). They found that specificity and sensitivity for with ADC maps was 96% and 94% respectively in diagnosing complete tears which was higher than the 87% and 50% specificity and sensitivity achieved when using T1 and T2 sequences with fat saturation. It was also found that the increase in specificity was statistically significant (P<0.01) but there was no statistically significant difference for sensitivity. Several studies investigated morphological changes on MRI to differentiate partial tears from complete tears

and although certain features such as wavy ligaments or ligament thinning are suggestive of partial tears, determination of partial tears still remains a challenge (47-51). The difficulty in differentiating partial and complete tears can be partially attributed to the edema that results from the injury, which appears as a hyperintense signal on T2-weighted images, obscuring ligament fibers. It was found that applying DWI to traumatic injuries can improve the differentiation of partial and complete tears and that ADC mapping may be more useful than morphological MRI alone in differentiating partial and complete ACL tears (46).

Pre- and post-treatment assessment

Even though MRI is the method of choice for diagnosis and follow up of soft-tissue masses (52), assessing therapy response can be difficult with conventional MRI techniques because tissues can demonstrate post therapeutic cytotoxic as well as edematous changes on T2-weighted and STIR images (53-58). In clinical practice, often times therapeutic response is based on assessment of tumor size. However, the lack of reduction in tumor size does not necessarily reflect a lack of response to treatment, which is true particularly for osteosarcomas or other tumors with a large proportion of matrix (59). Assessment of pretreatment and post-treatment ADC values may be of prognostic value with regard to outcomes and may also reflect treatment response (*Figure 3*). Biologically aggressive tumors with areas of necrosis may have higher ADC values associated with a worse outcome (60). Areas with increased ADC values post-treatment can indicate areas of tumor cells which underwent necrosis suggesting a positive response to therapy (61). Chemotherapy or radiation can result in necrosis or apoptosis of tumor cells, altering water diffusion and possibly allowing an earlier, non invasive assessment of treatment response (13,44,60). An animal study regarding osteosarcoma showed that DWI can effectively differentiate between necrotic and viable tissue (62). Following treatment, osteosarcoma tissue undergoes necrosis and results in hyaline fibrosis and granulation tissue (63) which enhance on contrast enhanced images. Therefore it is difficult to assess treatment response using conventional imaging techniques (59). DWI may be capable of differentiating these morphological changes which would have been otherwise obscured (64) in addition to quantifying the amount of necrosis (65-67).

Studies have shown that increasing ADC values following treatment of primary sarcomas of the bone correlates with
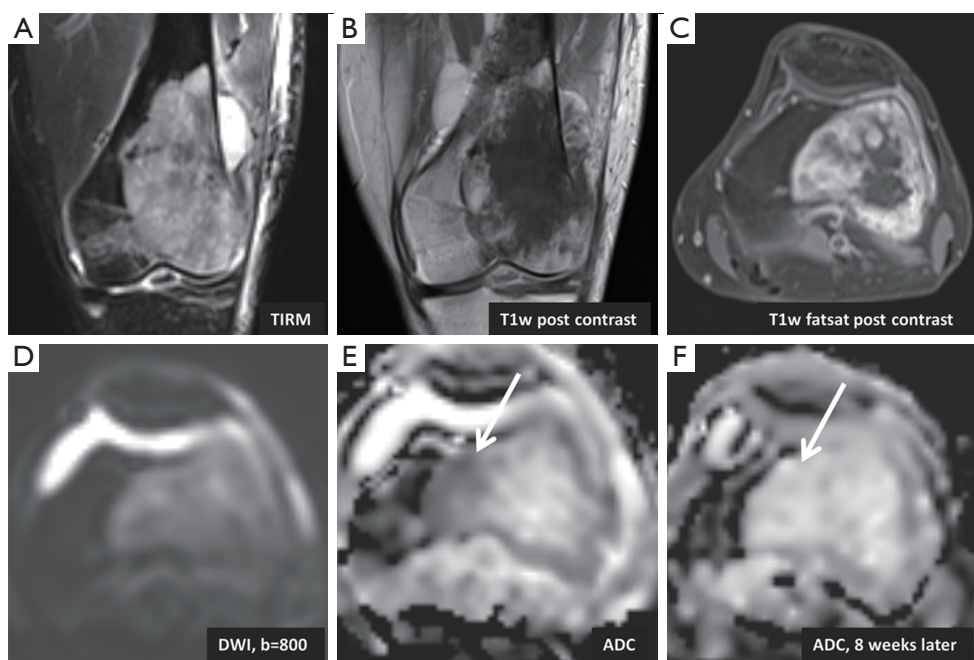

Figure 3 A 24-year-old female with osteosarcoma. (A-C) Conventional MRI reveals a solid osseous tumor mass in the left lateral femoral condyle with replacement of the normal marrow fat seen as bright T1 signal, an extraosseous soft tissue mass, and avid peripheral contrast enhancement; (D) DWI shows higher signal within the mass compared to normal bone in the medial condyle; the ADC values are low in the periphery of the mass, especially at its medial rim (E, white arrow); after initial chemotherapy of 8 weeks the ADC value of the medial rim has increased, indicating lower cellularity and therefore treatment response (F, white arrow). MRI, magnetic resonance imaging; DWI, diffusion-weighted imaging; ADC, apparent diffusion coefficients.

successful treatment (68,69). Necrosis in Ewing sarcomas and osteosarcomas has been recognized as a favorable prognostic factor following treatment (25). Osteosarcomas with greater than 90% necrosis post-treatment were associated with better outcomes (68). In one study (69), histologically confirmed necrotic areas were correlated with ADC maps demonstrated a mean ADC value of 2.3 (±0.2) whereas viable tumor had a mean ADC value of 0.8 (±0.2). Increased ADC values following treatment have also been described for vertebral metastatic disease, with a change from a high signal to a low signal relative to normal vertebral bodies on DWI indicating a positive response to therapy (61).

Differentiation of inflammatory, infectious and malignant processes

Osteomyelitis and malignancy can have overlapping features with both appearing as hyperintense on DWI with low ADC values (10,70). In bacterial (7) and tuberculous osteomyelitis (71), the increase in inflammatory cells in the bone marrow causes an increase in the diffusion-weighted signal with a corresponding decrease in ADC values. Protein in fluids can restrict water motion, hence infectious processes (e.g., abscesses) and endometriotic cysts may appear as having restricted diffusion (13). Pui *et al*. (10) found that when using an ADC cutoff value of cutoff of 1.02×10^{-3} mm^2/s gave a sensitivity and specificity of 60.26% and 66% respectively. The low sensitivity and specificity of DWI do not make it useful for differentiating infection and malignant processes in a clinical setting.

Assessment of abscesses can be difficult using DWI because as with tumors, their imaging features may change over time. Initially, the increased cellular and protein content of the abscess causes restricted diffusion, seen as hyperintensity on DWI. As time progresses, the T2 shine-through effect can become dominant as the center of an abscess begins to liquefy (72). One study (73) investigated a group of 50 patients who were suspected of having a soft-tissue abscess, 32 of which were intramuscular, 14 intra-abdominal, 1 periorbital and 3 breast abscesses. All patients had material aspirated as a

746

Bhojwani et al. Diffusion-weighted imaging in musculoskeletal radiology

confirmatory method. In this study DWI was shown to have a sensitivity and specificity of 92% and 80% respectively. Harish *et al*. (74) studied a group of eight patients and found that DWI, when used in conjunction with other imaging improved their confidence level for the diagnosis of abscess.

There have been a couple studies regarding the use of DWI for degenerative changes in the axial skeleton (6,7). Changes to the vertebral endplates may be the source of spine pain, in part due to disruption of diffusion of nutrients to the disc (75-78). Changes to the vertebral endplates are described according to their appearance on conventional T1 and T2 imaging using the Modic type classification system (76,79,80). One study investigated the use of DWI in differentiating endplate infectious causes from degenerative changes in the lumbar spine. ADC values in the infection group were found to be higher than in those with degenerative changes suggesting that DWI may be an additional tool for clinicians to differentiate between degenerative and infectious causes (9).

The reliance of intervertebral discs on diffusion for nutrients, not blood vessels, has suggested the possibility of using physical therapy in order to improve diffusion and ultimately clinical outcome. Applying mechanical pressure to the lumbar regions of patient significantly increased signal intensity on DWI (81). In a similar study (82), patients were asked to rate their pain after lumbar spine mobilization and those who reported immediate relief had a 4.7% increase in diffusion while those who did not respond to the treatment had a decrease of 1.6% in diffusion. The increased signal on DWI theoretically correlates with increased molecular level diffusion within the disc and can potentially be used as a method for monitoring therapy response, however, due to the small sample sizes, further studies would be required.

It is estimated that anywhere from 0.3% to 1.9% of the population is affected by inflammatory spondyloarthritis (SpA) (7,83,84). Both SpA and degenerative causes of lower back pain are common in young patients and must be distinguished (7). DWI has shown to be effective in differentiating between acute degenerative lesions and early inflammatory sacroiliitis (85). Dallaudière *et al*. (7) conducted a study using DWI to assess patients with inflammatory spondyloarthritis and type 1 Modic change. When the disc is undergoing inflammation, it is described as Modic type 1 changes corresponding to an inflammatory stage of disk degenerative disease (80). Axial active inflammatory lesions showed significantly higher ADC values (mean, 0.7888×10^{-3} mm^2/s)

compared to Modic changes (mean, 0.585×10^{-3} mm^2/s) and normal subchondral bone (mean, 0.445×10^{-3} mm^2/s). The difference in mean ADC values between subchondral bone and Modic changes was also statistically significant. Using a box-plot, the authors visually determined an optimal ADC cut-off value of 0.58×10^{-3} mm^2/s. A different study (86) found that ADC values correlated with active ankylosing spondylitis suggesting that DWI may be used to monitor patient response to therapy and disease progression. Detection of synovitis in rheumatoid arthritis can be facilitated using DWI (*Figure 4*).

Compression fractures

Atraumatic vertebral compression fractures are common in the elderly population and may be secondary to osteoporosis, metastatic disease or other pathologies, therefore it is clinically important to determine their underlying cause (88). Depending on the etiology, vertebral compression fractures may have distinct radiographic features allowing a diagnosis to be readily made. However, overlapping imaging characteristics exist (89). Osteoporotic fractures tend to be hypo- to isointense when compared to normal vertebral bodies and malignant fractures tend to be hyperintense on DWI. The hypointensity in osteoporotic fractures is secondary to the edema while the hyperintensity seen in metastatic fractures is due to densely packed tumor cells restricting water diffusion. In their study, Baur *et al*. (90) used a diffusion-weighted steady-state free precession (SSFP) sequence which was acquired with various diffusion weightings. Reduction of false-positives was achieved by increasing the diffusion weighting, changing hyperintense osteoporotic fractures to a more hypointense appearance, a feature not seen in malignant compression fractures (90).

Zhou *et al*. (91) investigated the use of ADC maps and found that benign fractures showed higher ADC values when compared to metastatic fractures, with values of $(3.2 \pm 0.5) \times 10^{-3}$ and $(1.9 \pm 0.3) \times 10^{-4}$ mm^2/s respectively. Although, this result has been found in several other studies (10,61,92,93), there is overlap between ADC values depending on imaging protocols, and no cut-off can be determined at this point (13). Again, tumors tend to demonstrate lower ADC values due to their cellularity in the early stages of growth while in later stages when necrosis predominates, increased ADC values may be seen. The DWI results should be combined with morphologic MR findings and other functional imaging modalities such as PET, for instance when using the novel hybrid imaging
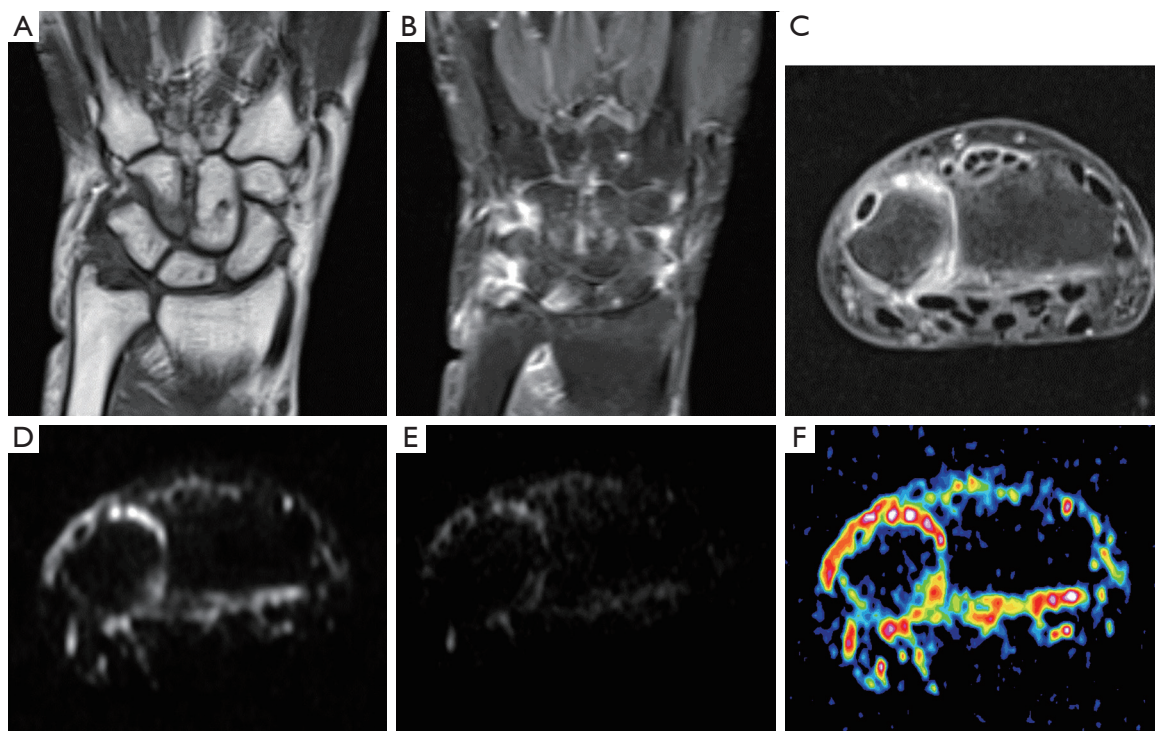
Figure 4 A 74-year-old female with late-onset rheumatoid arthritis with the following MR images: (A) T1w coronal; (B) T1w fat suppressed post gadolinium coronal; (C) T1w fat suppressed post gadolinium axial; (D) DWI with b=50 axial; (E) DWI with b=800 axial and corresponding ADC map color coded axial. Morphologic findings include radiocarpal and distal radioulnar joint space narrowing as well as enhancement of the synovium. Please note that although some authors (87) advocate DWI as a novel non-invasive approach to contrast-free imaging of synovitis, the signal hyperintensity on DWI with corresponding high ADC-values reflects mainly T2-shine-through-effects and does not represent true diffusion restriction. DWI, diffusion-weighted imaging; ADC, apparent diffusion coefficients.

technology PET/MRI (*Figure 5*). False-negatives can arise when the lesions are sclerotic (13) demonstrating low signal on conventional MRI and DWI due to the increased fibrotic content of the lesion.

Limitations of DWI

DWI has limitations including susceptibility, motion, and arterial pulsation artifacts, requiring imaging protocols modifications in order to limit the amount of noise (59,72). Diffusion MRI is more sensitive to motion in comparison to other sequences, a problem which has been minimized by the use of echo-planar imaging. Echo-planar imaging, however, provides lower spatial resolution images and is more susceptible to eddy currents (94). These artifacts from eddy currents are introduced at bone-tissue and air-tissue interfaces (95). Patient motion can cause voxels to change position, an especially important consideration when taking multiple images at different b-values to calculate ADC

maps. Calculating ADC maps also requires the assumption that voxels have a certain size when in fact they vary according to the local diffusion gradient strength (94). At times, depending on the imaging technique used it may not be possible to calculate an ADC map, such as with a SSFP sequence (90).

Pitfalls of DWI

There are several challenges that are associated with the creation and interpretation of DWI. The guidelines for choosing a region of interest are not well-established even though tumors are often heterogeneous. As discussed, post-therapy with mixed viable tumor and areas of necrosis lead to inter-reader differences (12). One study using multiple, small regions of interest and minimum ADC values, found extensive variability within the tumor (14). The usage of minimum ADC values is suggested because the regions of interest with the lowest ADC values theoretically correlate
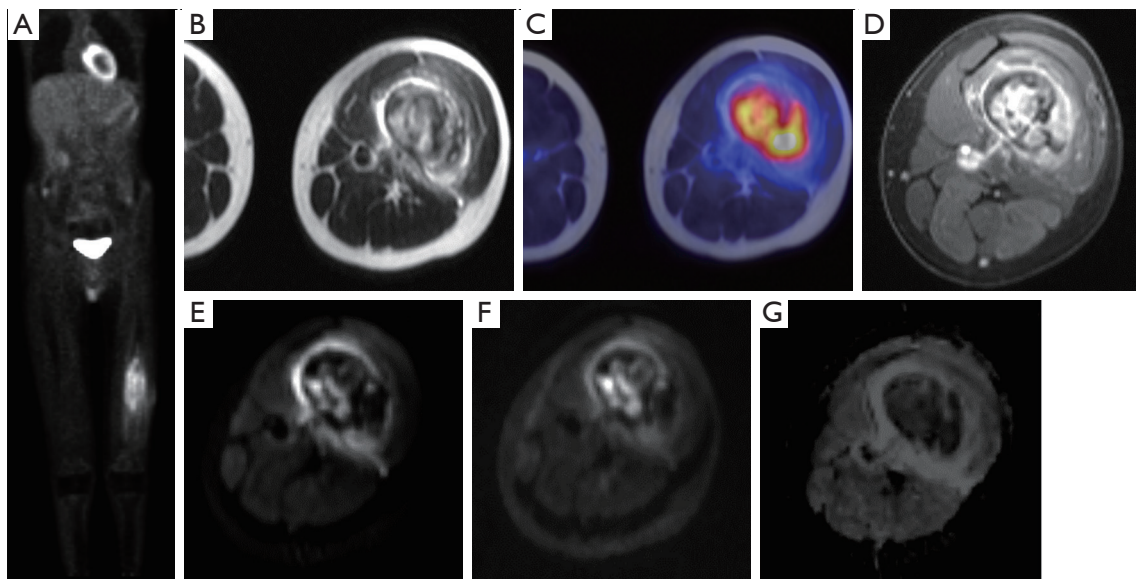
 Quant Imaging Med Surg 2015;5(5):740-753

Figure 5 A 16-year-old male patient with osteosarcoma of the mid femoral shaft who was imaged with whole-body FDG-PET/MRI (Siemens, Biograph mMR). PET acquisition was performed 67 min post FDG injection. The following images are provided: (A) whole body PET maximum-intensity projection; (B) T2w HASTE axial; (C) fusion of T2w HASTE axial and FDG-PET axial; (D) T1w VIBE axial; (E) DWI with b=50 axial; (F) DWI with b=800 axial; (G) corresponding ADC map axial. The FDG avid malignancy is seen on AP planar whole body image within the left femoral diaphysis. Within the medial aspect of the tumor there is increased signal on T2WI, high b value DWI, and corresponding low signal on ADC map consistent with area of high grade tumor cellularity. PET and DWI images demonstrate the marked heterogeneity of the tumor with necrotic areas and other highly cellular tumor. PET, positron emission tomography; MRI, magnetic resonance imaging; DWI, diffusion-weighted imaging; ADC, apparent diffusion coefficients; HASTE, half-Fourier acquisition single-shot; VIBE, volumetric interpolated breath-hold examination.

Table 1 Clinically important pitfalls in DWI

Pitfalls associated with DWI
T2-shine through effect
Non-standardized MRI and image acquisition techniques
Lack of collaboration between vendors
Different imaging protocols and processing models (e.g., mono-exponential modeling)
No pre-defined b values for a given tumor or its location (61)
Perfusion and diffusion components contributing to varying DWI signal, adding to the complexity in interpretation (13)

DWI, diffusion-weighted imaging; MRI, magnetic resonance imaging.

well with regions of high cellularity (14) and can possibly indicate regions which did not respond to therapy.

B values are influenced by the gyromagnetic ratio, gradient strength, diffusion gradient duration, and time between diffusion gradient pulses, all of which influence the ADC values (12). Taking into consideration the variation in MRI specifications between vendors and imaging protocols used in different institutions, it is challenging to standardize b values and the calculated ADC values. Depending on the location of the tumor, artifacts may appear at bone-tissue or air-tissue interfaces therefore modified imaging protocols may be required (95). Tumors can also appear similar to simple fluid on T2-weighted images due to the T2-shine through effect (64). Ideally, DWI should be correlated with ADC maps (96). *Table 1* lists clinically important pitfalls associated with DWI.

Conclusions and future directions

DWI has been shown to add value in several areas by being part of the multi-parametric MRI approach, even though quantitative values tend to overlap. Investigations into the clinical applications regarding monitoring tumor burden or whole-body imaging are still at an early stage. A challenge that DWI faces is standardization of imaging protocols allowing for better comparisons across studies. Therefore, initiatives like the Quantitative Imaging Biomarkers Alliance (QIBA) organized by RSNA are very promising. It is also uncertain whether therapies other than those which cause apoptosis or ischemia and essentially associated with alterations in cellularity, are capable of being measured by DWI (60).

Currently, studies have shown that DWI can be used for various musculoskeletal pathologies and is showing promising results in a variety of applications. It has been demonstrated that MRI can be useful in differentiating partial and complete ACL tears (46). The diffusion properties of tumors pre- and post-treatment can be used to assess the prognosis of patients who have soft-tissue tumors (59,60). The effects of increased cellularity of tumors on diffusion can also be exploited to localize soft-tissue tumors and bone lesions (26). The use of DWI in differentiating infectious from malignant causes is limited due to overlapping imaging characteristics (10) but has shown utility in differentiating osteoporotic and metastatic compression fractures (5). It will be crucial to correlate DWI with morphology on MRI and other functional techniques, such as PET as suggested when applying PET/MRI for musculoskeletal applications (97,98).

Acknowledgements

Footnote

Conflicts of Interest: The authors have no conflicts of interest to declare.

References

1. Le Bihan D, Breton E, Lallemand D, Grenier P, Cabanis E, Laval-Jeantet M. MR imaging of intravoxel incoherent motions: application to diffusion and perfusion in neurologic disorders. Radiology 1986;161:401-7.

2. Mintorovitch J, Moseley ME, Chileuitt L, Shimizu H, Cohen Y, Weinstein PR. Comparison of diffusion- and T2-weighted MRI for the early detection of cerebral ischemia and reperfusion in rats. Magn Reson Med 1991;18:39-50.

3. Chien D, Kwong KK, Gress DR, Buonanno FS, Buxton RB, Rosen BR. MR diffusion imaging of cerebral infarction in humans. AJNR Am J Neuroradiol 1992;13:1097-102; discussion 1103-5.

4. Warach S, Gaa J, Siewert B, Wielopolski P, Edelman RR. Acute human stroke studied by whole brain echo planar diffusion-weighted magnetic resonance imaging. Ann Neurol 1995;37:231-41.

5. Baur A, Stäbler A, Brüning R, Bartl R, Krödel A, Reiser M, Deimling M. Diffusion-weighted MR imaging of bone marrow: differentiation of benign versus pathologic compression fractures. Radiology 1998;207:349-56.

6. Kealey SM, Aho T, Delong D, Barboriak DP, Provenzale JM, Eastwood JD. Assessment of apparent diffusion coefficient in normal and degenerated intervertebral lumbar disks: initial experience. Radiology 2005;235:569-74.

7. Dallaudière B, Dautry R, Preux PM, Perozziello A, Lincot J, Schouman-Claeys E, Serfaty JM. Comparison of apparent diffusion coefficient in spondylarthritis axial active inflammatory lesions and type 1 Modic changes. Eur J Radiol 2014;83:366-70.

8. Baur A, Huber A, Arbogast S, Dürr HR, Zysk S, Wendtner C, Deimling M, Reiser M. Diffusion-weighted imaging of tumor recurrencies and posttherapeutical soft-tissue changes in humans. Eur Radiol 2001;11:828-33.

9. Eguchi Y, Ohtori S, Yamashita M, Yamauchi K, Suzuki M, Orita S, Kamoda H, Arai G, Ishikawa T, Miyagi M, Ochiai N, Kishida S, Masuda Y, Ochi S, Kikawa T, Takaso M, Aoki Y, Inoue G, Toyone T, Takahashi K. Diffusion magnetic resonance imaging to differentiate degenerative from infectious endplate abnormalities in the lumbar spine. Spine (Phila Pa 1976) 2011;36:E198-202.

10. Pui MH, Mitha A, Rae WI, Corr P. Diffusion-weighted magnetic resonance imaging of spinal infection and malignancy. J Neuroimaging 2005;15:164-70.

11. Yakushiji T, Oka K, Sato H, Yorimitsu S, Fujimoto T, Yamashita Y, Mizuta H. Characterization of chondroblastic osteosarcoma: gadolinium-enhanced versus diffusion-weighted MR imaging. J Magn Reson Imaging 2009;29:895-900.

12. Subhawong TK, Jacobs MA, Fayad LM. Insights into quantitative diffusion-weighted MRI for musculoskeletal tumor imaging. AJR Am J Roentgenol 2014;203:560-72.

13. Khoo MM, Tyler PA, Saifuddin A, Padhani AR. Diffusion-

weighted imaging (DWI) in musculoskeletal MRI: a critical review. Skeletal Radiol 2011;40:665-81.

14. Oka K, Yakushiji T, Sato H, Yorimitsu S, Hayashida Y, Yamashita Y, Mizuta H. Ability of diffusion-weighted imaging for the differential diagnosis between chronic expanding hematomas and malignant soft tissue tumors. J Magn Reson Imaging 2008;28:1195-200.

15. Einarsdóttir H, Karlsson M, Wejde J, Bauer HC. Diffusion-weighted MRI of soft tissue tumours. Eur Radiol 2004;14:959-63.

16. Razek A, Nada N, Ghaniem M, Elkhamary S. Assessment of soft tissue tumours of the extremities with diffusion echoplanar MR imaging. Radiol Med 2012;117:96-101.

17. Subhawong TK, Durand DJ, Thawait GK, Jacobs MA, Fayad LM. Characterization of soft tissue masses: can quantitative diffusion weighted imaging reliably distinguish cysts from solid masses? Skeletal Radiol 2013;42:1583-92.

18. van Rijswijk CS, Kunz P, Hogendoorn PC, Taminiau AH, Doornbos J, Bloem JL. Diffusion-weighted MRI in the characterization of soft-tissue tumors. J Magn Reson Imaging 2002;15:302-7.

19. Maeda M, Matsumine A, Kato H, Kusuzaki K, Maier SE, Uchida A, Takeda K. Soft-tissue tumors evaluated by line-scan diffusion-weighted imaging: influence of myxoid matrix on the apparent diffusion coefficient. J Magn Reson Imaging 2007;25:1199-204.

20. Alibek S, Cavallaro A, Aplas A, Uder M, Staatz G. Diffusion weighted imaging of pediatric and adolescent malignancies with regard to detection and delineation: initial experience. Acad Radiol 2009;16:866-71.

21. Takahara T, Imai Y, Yamashita T, Yasuda S, Nasu S, Van Cauteren M. Diffusion weighted whole body imaging with background body signal suppression (DWIBS): technical improvement using free breathing, STIR and high resolution 3D display. Radiat Med 2004;22:275-82.

22. Kwee TC, Takahara T, Ochiai R, Nievelstein RA, Luijten PR. Diffusion-weighted whole-body imaging with background body signal suppression (DWIBS): features and potential applications in oncology. Eur Radiol 2008;18:1937-52.

23. Gutzeit A, Doert A, Froehlich JM, Eckhardt BP, Meili A, Scherr P, Schmid DT, Graf N, von Weymarn CA, Willemse EM, Binkert CA. Comparison of diffusion-weighted whole body MRI and skeletal scintigraphy for the detection of bone metastases in patients with prostate or breast carcinoma. Skeletal Radiol 2010;39:333-43.

24. Goudarzi B, Kishimoto R, Komatsu S, Ishikawa H, Yoshikawa K, Kandatsu S, Obata T. Detection of bone metastases using diffusion weighted magnetic resonance imaging: comparison with (11)C-methionine PET and bone scintigraphy. Magn Reson Imaging 2010;28:372-9.

25. Gould P. Medical isotope shortage reaches crisis level. Nature 2009;460:312-3.

26. Wu LM, Gu HY, Zheng J, Xu X, Lin LH, Deng X, Zhang W, Xu JR. Diagnostic value of whole-body magnetic resonance imaging for bone metastases: a systematic review and meta-analysis. J Magn Reson Imaging 2011;34:128-35.

27. Koh DM, Blackledge M, Padhani AR, Takahara T, Kwee TC, Leach MO, Collins DJ. Whole-body diffusion-weighted MRI: tips, tricks, and pitfalls. AJR Am J Roentgenol 2012;199:252-62.

28. Jacobs MA, Pan L, Macura KJ. Whole-body diffusion-weighted and proton imaging: a review of this emerging technology for monitoring metastatic cancer. Semin Roentgenol 2009;44:111-22.

29. Pearce T, Philip S, Brown J, Koh DM, Burn PR. Bone metastases from prostate, breast and multiple myeloma: differences in lesion conspicuity at short-tau inversion recovery and diffusion-weighted MRI. Br J Radiol 2012;85:1102-6.

30. Fischer MA, Nanz D, Hany T, Reiner CS, Stolzmann P, Donati OF, Breitenstein S, Schneider P, Weishaupt D, von Schulthess GK, Scheffel H. Diagnostic accuracy of whole-body MRI/DWI image fusion for detection of malignant tumours: a comparison with PET/CT. Eur Radiol 2011;21:246-55.

31. Hauben EI, Weeden S, Pringle J, Van Marck EA, Hogendoorn PC. Does the histological subtype of high-grade central osteosarcoma influence the response to treatment with chemotherapy and does it affect overall survival? A study on 570 patients of two consecutive trials of the European Osteosarcoma Intergroup. Eur J Cancer 2002;38:1218-25.

32. Geirnaerdt MJ, Bloem JL, Eulderink F, Hogendoorn PC, Taminiau AH. Cartilaginous tumors: correlation of gadolinium-enhanced MR imaging and histopathologic findings. Radiology 1993;186:813-7.

33. Dorfman HD, Czerniak B. Bone cancers. Cancer 1995;75:203-10.

34. Bacci G, Bertoni F, Longhi A, Ferrari S, Forni C, Biagini R, Bacchini P, Donati D, Manfrini M, Bernini G, Lari S. Neoadjuvant chemotherapy for high-grade central osteosarcoma of the extremity. Histologic response to preoperative chemotherapy correlates with histologic subtype of the tumor. Cancer 2003;97:3068-75.

35. Geirnaerdt MJ, Bloem JL, van der Woude HJ, Taminiau

AH, Nooy MA, Hogendoorn PC. Chondroblastic osteosarcoma: characterisation by gadolinium-enhanced MR imaging correlated with histopathology. Skeletal Radiol 1998;27:145-53.

36. De Beuckeleer LH, De Schepper AM, Ramon F, Somville J. Magnetic resonance imaging of cartilaginous tumors: a retrospective study of 79 patients. Eur J Radiol 1995;21:34-40.

37. Hwang S, Panicek DM. Magnetic resonance imaging of bone marrow in oncology, Part 1. Skeletal Radiol 2007;36:913-20.

38. Nonomura Y, Yasumoto M, Yoshimura R, Haraguchi K, Ito S, Akashi T, Ohashi I. Relationship between bone marrow cellularity and apparent diffusion coefficient. J Magn Reson Imaging 2001;13:757-60.

39. Tang GY, Lv ZW, Tang RB, Liu Y, Peng YF, Li W, Cheng YS. Evaluation of MR spectroscopy and diffusion-weighted MRI in detecting bone marrow changes in postmenopausal women with osteoporosis. Clin Radiol 2010;65:377-81.

40. Yasumoto M, Nonomura Y, Yoshimura R, Haraguchi K, Ito S, Ohashi I, Shibuya H. MR detection of iliac bone marrow involvement by malignant lymphoma with various MR sequences including diffusion-weighted echo-planar imaging. Skeletal Radiol 2002;31:263-9.

41. Reid JD, Kommareddi S, Lankerani M, Park MC. Chronic expanding hematomas. A clinicopathologic entity. JAMA 1980;244:2441-2.

42. Aoki T, Nakata H, Watanabe H, Maeda H, Toyonaga T, Hashimoto H, Nakamura T. The radiological findings in chronic expanding hematoma. Skeletal Radiol 1999;28:396-401.

43. Kang BK, Na DG, Ryoo JW, Byun HS, Roh HG, Pyeun YS. Diffusion-weighted MR imaging of intracerebral hemorrhage. Korean J Radiol 2001;2:183-91.

44. Costa FM, Ferreira EC, Vianna EM. Diffusion-weighted magnetic resonance imaging for the evaluation of musculoskeletal tumors. Magn Reson Imaging Clin N Am 2011;19:159-80.

45. Lee JC, Thomas JM, Phillips S, Fisher C, Moskovic E. Aggressive fibromatosis: MRI features with pathologic correlation. AJR Am J Roentgenol 2006;186:247-54.

46. Delin C, Silvera S, Coste J, Thelen P, Lefevre N, Ehkirch FP, Le Couls V, Oudjit A, Radier C, Legmann P. Reliability and diagnostic accuracy of qualitative evaluation of diffusion-weighted MRI combined with conventional MRI in differentiating between complete and partial anterior cruciate ligament tears. Eur Radiol 2013;23:845-54.

47. Chen WT, Shih TT, Tu HY, Chen RC, Shau WY. Partial and complete tear of the anterior cruciate ligament. Acta Radiol 2002;43:511-6.

48. Lawrance JA, Ostlere SJ, Dodd CA. MRI diagnosis of partial tears of the anterior cruciate ligament. Injury 1996;27:153-5.

49. Tsai KJ, Chiang H, Jiang CC. Magnetic resonance imaging of anterior cruciate ligament rupture. BMC Musculoskelet Disord 2004;5:21.

50. Umans H, Wimpfheimer O, Haramati N, Applbaum YH, Adler M, Bosco J. Diagnosis of partial tears of the anterior cruciate ligament of the knee: value of MR imaging. AJR Am J Roentgenol 1995;165:893-7.

51. Yao L, Gentili A, Petrus L, Lee JK. Partial ACL rupture: an MR diagnosis? Skeletal Radiol 1995;24:247-51.

52. Walker EA, Salesky JS, Fenton ME, Murphey MD. Magnetic resonance imaging of malignant soft tissue neoplasms in the adult. Radiol Clin North Am 2011;49:1219-34, vi.

53. Weinmann HJ, Brasch RC, Press WR, Wesbey GE. Characteristics of gadolinium-DTPA complex: a potential NMR contrast agent. AJR Am J Roentgenol 1984;142:619-24.

54. Vanel D, Shapeero LG, De Baere T, Gilles R, Tardivon A, Genin J, Guinebretière JM. MR imaging in the follow-up of malignant and aggressive soft-tissue tumors: results of 511 examinations. Radiology 1994;190:263-8.

55. Reddick WE, Bhargava R, Taylor JS, Meyer WH, Fletcher BD. Dynamic contrast-enhanced MR imaging evaluation of osteosarcoma response to neoadjuvant chemotherapy. J Magn Reson Imaging 1995;5:689-94.

56. Verstraete KL, De Deene Y, Roels H, Dierick A, Uyttendaele D, Kunnen M. Benign and malignant musculoskeletal lesions: dynamic contrast-enhanced MR imaging--parametric "first-pass" images depict tissue vascularization and perfusion. Radiology 1994;192:835-43.

57. Roberts TP. Physiologic measurements by contrast-enhanced MR imaging: expectations and limitations. J Magn Reson Imaging 1997;7:82-90.

58. Erlemann R. Dynamic, gadolinium-enhanced MR imaging to monitor tumor response to chemotherapy. Radiology 1993;186:904-5.

59. Bley TA, Wieben O, Uhl M. Diffusion-weighted MR imaging in musculoskeletal radiology: applications in trauma, tumors, and inflammation. Magn Reson Imaging Clin N Am 2009;17:263-75.

60. Padhani AR, Liu G, Koh DM, Chenevert TL, Thoeny HC, Takahara T, Dzik-Jurasz A, Ross BD, Van

Cauteren M, Collins D, Hammoud DA, Rustin GJ, Taouli B, Choyke PL. Diffusion-weighted magnetic resonance imaging as a cancer biomarker: consensus and recommendations. Neoplasia 2009;11:102-25.

61. Byun WM, Shin SO, Chang Y, Lee SJ, Finsterbusch J, Frahm J. Diffusion-weighted MR imaging of metastatic disease of the spine: assessment of response to therapy. AJNR Am J Neuroradiol 2002;23:906-12.

62. Lang P, Wendland MF, Saeed M, Gindele A, Rosenau W, Mathur A, Gooding CA, Genant HK. Osteogenic sarcoma: noninvasive in vivo assessment of tumor necrosis with diffusion-weighted MR imaging. Radiology 1998;206:227-35.

63. Roberge D, Skamene T, Nahal A, Turcotte RE, Powell T, Freeman C. Radiological and pathological response following pre-operative radiotherapy for soft-tissue sarcoma. Radiother Oncol 2010;97:404-7.

64. Fayad LM, Jacobs MA, Wang X, Carrino JA, Bluemke DA. Musculoskeletal tumors: how to use anatomic, functional, and metabolic MR techniques. Radiology 2012;265:340-56.

65. Chenevert TL, Meyer CR, Moffat BA, Rehemtulla A, Mukherji SK, Gebarski SS, Quint DJ, Robertson PL, Lawrence TS, Junck L, Taylor JM, Johnson TD, Dong Q, Muraszko KM, Brunberg JA, Ross BD. Diffusion MRI: a new strategy for assessment of cancer therapeutic efficacy. Mol Imaging 2002;1:336-43.

66. Dudeck O, Zeile M, Pink D, Pech M, Tunn PU, Reichardt P, Ludwig WD, Hamm B. Diffusion-weighted magnetic resonance imaging allows monitoring of anticancer treatment effects in patients with soft-tissue sarcomas. J Magn Reson Imaging 2008;27:1109-13.

67. Zhao M, Pipe JG, Bonnett J, Evelhoch JL. Early detection of treatment response by diffusion-weighted 1H-NMR spectroscopy in a murine tumour in vivo. Br J Cancer 1996;73:61-4.

68. Hayashida Y, Yakushiji T, Awai K, Katahira K, Nakayama Y, Shimomura O, Kitajima M, Hirai T, Yamashita Y, Mizuta H. Monitoring therapeutic responses of primary bone tumors by diffusion-weighted image: Initial results. Eur Radiol 2006;16:2637-43.

69. Uhl M, Saueressig U, van Buiren M, Kontny U, Niemeyer C, Köhler G, Ilyasov K, Langer M. Osteosarcoma: preliminary results of in vivo assessment of tumor necrosis after chemotherapy with diffusion- and perfusion-weighted magnetic resonance imaging. Invest Radiol 2006;41:618-23.

70. Chan JH, Peh WC, Tsui EY, Chau LF, Cheung KK, Chan

KB, Yuen MK, Wong ET, Wong KP. Acute vertebral body compression fractures: discrimination between benign and malignant causes using apparent diffusion coefficients. Br J Radiol 2002;75:207-14.

71. Stäbler A, Doma AB, Baur A, Krüger A, Reiser MF. Reactive bone marrow changes in infectious spondylitis: quantitative assessment with MR imaging. Radiology 2000;217:863-8.

72. Herneth AM, Ringl H, Memarsadeghi M, Fueger B, Friedrich KM, Krestan C, Imhof H. Diffusion weighted imaging in osteoradiology. Top Magn Reson Imaging 2007;18:203-12.

73. Unal O, Koparan HI, Avcu S, Kalender AM, Kisli E. The diagnostic value of diffusion-weighted magnetic resonance imaging in soft tissue abscesses. Eur J Radiol 2011;77:490-4.

74. Harish S, Chiavaras MM, Kotnis N, Rebello R. MR imaging of skeletal soft tissue infection: utility of diffusion-weighted imaging in detecting abscess formation. Skeletal Radiol 2011;40:285-94.

75. Bogduk N, Twomey LT. Clinical Anatomy of the Lumbar Spine. London: Churchill Livingstone, 1987.

76. Mitra D, Cassar-Pullicino VN, McCall IW.Longitudinal study of vertebral type-1 end-plate changes on MR of the lumbar spine. Eur Radiol 2004;14:1574-81.

77. Moore RJ. The vertebral endplate: disc degeneration, disc regeneration. Eur Spine J 2006;15 Suppl 3:S333-7.

78. Rajasekaran S, Babu JN, Arun R, Armstrong BR, Shetty AP, Murugan S. ISSLS prize winner: A study of diffusion in human lumbar discs: a serial magnetic resonance imaging study documenting the influence of the endplate on diffusion in normal and degenerate discs. Spine (Phila Pa 1976) 2004;29:2654-67.

79. Jones A, Clarke A, Freeman BJ, Lam KS, Grevitt MP. The Modic classification: inter- and intraobserver error in clinical practice. Spine (Phila Pa 1976) 2005;30:1867-9.

80. Modic MT, Steinberg PM, Ross JS, Masaryk TJ, Carter JR. Degenerative disk disease: assessment of changes in vertebral body marrow with MR imaging. Radiology 1988;166:193-9.

81. Beattie PF, Donley JW, Arnot CF, Miller R. The change in the diffusion of water in normal and degenerative lumbar intervertebral discs following joint mobilization compared to prone lying. J Orthop Sports Phys Ther 2009;39:4-11.

82. Beattie PF, Donley JW, Arnot CF, Miller R. The immediate reduction in low back pain intensity following lumbar joint mobilization and prone press-ups is associated with increased diffusion of water in the

L5-S1 intervertebral disc. J Orthop Sports Phys Ther 2010;40:256-64.

83. Sieper J, Rudwaleit M, Khan MA, Braun J. Concepts and epidemiology of spondyloarthritis. Best Pract Res Clin Rheumatol 2006;20:401-17.

84. Saraux A, Guillemin F, Guggenbuhl P, Roux CH, Fardellone P, Le Bihan E, Cantagrel A, Chary-Valckenaere I, Euller-Ziegler L, Flipo RM, Juvin R, Behier JM, Fautrel B, Masson C, Coste J. Prevalence of spondyloarthropathies in France: 2001. Ann Rheum Dis 2005;64:1431-5.

85. Bozgeyik Z, Ozgocmen S, Kocakoc E. Role of diffusion-weighted MRI in the detection of early active sacroiliitis. AJR Am J Roentgenol 2008;191:980-6.

86. Gaspersic N, Sersa I, Jevtic V, Tomsic M, Praprotnik S. Monitoring ankylosing spondylitis therapy by dynamic contrast-enhanced and diffusion-weighted magnetic resonance imaging. Skeletal Radiol 2008;37:123-31.

87. Li X, Liu X, Du X, Ye Z. Diffusion-weighted MR imaging for assessing synovitis of wrist and hand in patients with rheumatoid arthritis: a feasibility study. Magn Reson Imaging 2014;32:350-3.

88. Compston J. Osteoporosis: social and economic impact. Radiol Clin North Am 2010;48:477-82.

89. Leeds N, Zhou X, McKinnon G, et al. Diffusion imaging of the spine: quantitative ADC mapping explaining signal change. Proc Am Soc Neuroradiol 2000;1:12.

90. Baur A, Huber A, Ertl-Wagner B, Dürr R, Zysk S, Arbogast S, Deimling M, Reiser M. Diagnostic value of increased diffusion weighting of a steady-state free precession sequence for differentiating acute benign osteoporotic fractures from pathologic vertebral compression fractures. AJNR Am J Neuroradiol 2001;22:366-72.

91. Zhou XJ, Leeds NE, McKinnon GC, Kumar AJ. Characterization of benign and metastatic vertebral compression fractures with quantitative diffusion MR imaging. AJNR Am J Neuroradiol 2002;23:165-70.

92. Raya JG, Dietrich O, Reiser MF, Baur-Melnyk A. Methods and applications of diffusion imaging of vertebral bone marrow. J Magn Reson Imaging 2006;24:1207-20.

93. Byun WM, Jang HW, Kim SW, Jang SH, Ahn SH, Ahn MW. Diffusion-weighted magnetic resonance imaging of sacral insufficiency fractures: comparison with metastases of the sacrum. Spine (Phila Pa 1976) 2007;32:E820-4.

94. Le Bihan D, Poupon C, Amadon A, Lethimonnier F. Artifacts and pitfalls in diffusion MRI. J Magn Reson Imaging 2006;24:478-88.

95. MacKenzie JD, Gonzalez L, Hernandez A, Ruppert K, Jaramillo D. Diffusion-weighted and diffusion tensor imaging for pediatric musculoskeletal disorders. Pediatr Radiol 2007;37:781-8.

96. Burdette JH, Elster AD, Ricci PE. Acute cerebral infarction: quantification of spin-density and T2 shine-through phenomena on diffusion-weighted MR images. Radiology 1999;212:333-9.

97. Partovi S, Kohan AA, Zipp L, Faulhaber P, Kosmas C, Ros PR, Robbin MR. Hybrid PET/MR imaging in two sarcoma patients - clinical benefits and implications for future trials. Int J Clin Exp Med 2014;7:640-8. eCollection 2014.

98. Partovi S, Chalian M, Fergus N, Kosmas C, Zipp L, Mansoori B, Ros PR, Robbin MR. Magnetic resonance/ positron emission tomography (MR/PET) oncologic applications: bone and soft tissue sarcoma. Semin Roentgenol 2014;49:345-52.